

---

This is an electronic reprint of the original article.  
This reprint may differ from the original in pagination and typographic detail.

Nyrhinen, Mikko J.; Souza, Victor H.; Ilmoniemi, Risto J.; Lin, Fa Hsuan  
**Acoustic noise generated by TMS in typical environment and inside an MRI scanner**

*Published in:*  
Brain Stimulation

*DOI:*  
[10.1016/j.brs.2024.02.006](https://doi.org/10.1016/j.brs.2024.02.006)

Published: 01/03/2024

*Document Version*  
Publisher's PDF, also known as Version of record

*Published under the following license:*  
CC BY

*Please cite the original version:*  
Nyrhinen, M. J., Souza, V. H., Ilmoniemi, R. J., & Lin, F. H. (2024). Acoustic noise generated by TMS in typical environment and inside an MRI scanner. *Brain Stimulation*, 17(2), 184-193.  
<https://doi.org/10.1016/j.brs.2024.02.006>

---

This material is protected by copyright and other intellectual property rights, and duplication or sale of all or part of any of the repository collections is not permitted, except that material may be duplicated by you for your research use or educational purposes in electronic or print form. You must obtain permission for any other use. Electronic or print copies may not be offered, whether for sale or otherwise to anyone who is not an authorised user.



# Acoustic noise generated by TMS in typical environment and inside an MRI scanner

Mikko J. Nyrhinen<sup>a,b,\*</sup>, Victor H. Souza<sup>a,b,c</sup>, Risto J. Ilmoniemi<sup>a</sup>, Fa-Hsuan Lin<sup>a,d</sup>

<sup>a</sup> Department of Neuroscience and Biomedical Engineering, Aalto University, Espoo, Finland

<sup>b</sup> Aalto Neuroimaging, Aalto University School of Science, Espoo, Finland

<sup>c</sup> School of Physiotherapy, Federal University of Juiz de Fora, Juiz de Fora, Brazil

<sup>d</sup> Department of Medical Biophysics, University of Toronto, Toronto, Canada

## ABSTRACT

**Background:** The operation of a transcranial magnetic stimulation (TMS) coil produces high-intensity impulse sounds. In TMS, a magnetic field is generated by a short-duration pulse in the range of thousands of amperes in the TMS coil. When placed in a strong magnetic field, such as inside a magnetic resonance imaging (MRI) bore, the interaction of the magnetic field and the current in the TMS coil can cause strong forces on the coil casing. The strengths of these forces depend on the coil orientation in the main magnetic field ( $B_0$ ). Part of the energy in this process is dissipated in the form of acoustic noise.

**Objective:** Our objective was to measure the sound pressure levels (SPL) of TMS “click” sounds created by commercial TMS stimulators and coils in a typical environment and inside a 3-T MRI scanner and advance the knowledge of the acoustic behaviour of TMS to safely conduct TMS alone as well as concurrently with functional MRI (fMRI).

**Methods:** We report SPL measurements of two commercial MRI-compatible TMS systems in the 3-T  $B_0$  field of an MRI scanner and in the earth’s magnetic field. Also, we present the acoustic noise measurements of four commercial TMS stimulators and three different TMS coils in a typical operational environment without the  $B_0$  field.

**Results:** The maximum peak SPL measured was 158 dB(C) inside the 3-T MRI scanner. Outside the scanner, the maximum peak SPL was 117 dB(C). Inside the scanner, the peak SPL increased by 21–45 dB(C) depending on the stimulator and the orientation of the electric field relative to the  $B$  field.

**Conclusions:** Hearing protection is obligatory during concurrent TMS–fMRI experiments and highly recommended during any TMS experiment. The manufacturing of quieter TMS systems is encouraged to reduce the risk of hearing damage and other unwanted effects.

## 1. Introduction

The operation of a transcranial magnetic stimulation (TMS) coil produces high-intensity impulse sounds in the form of clicks [1–3]. In TMS, a transient magnetic field is generated by a short-duration current pulse of thousands of amperes going through the wires of a TMS coil, producing strong forces in the wires and a consequent click sound. The instantaneous sound pressure level (SPL) of the click sound may exceed 140 dB [3]. When placed in a strong magnetic field, such as inside the bore of a magnetic resonance imaging (MRI) scanner, forces can be even stronger. These forces depend on the TMS coil orientation relative to the static magnetic field ( $B_0$ ) [4]. Exposure to loud acoustic noise can cause severe effects such as permanent hearing loss or tinnitus [5]. In order to perform safely a concurrent TMS with functional magnetic resonance imaging (fMRI) experiment [4,6], the SPL generated by the TMS coil must be quantitatively characterized.

In EU legislation, the hard exposure limits for workplaces, measured

inside the ear canal that may not be exceeded, are 140 dB(C) (200 Pa) and 87 dB(A) (Fig. 1) for the peak SPL and the daily noise exposure ( $L_{EX,8h}$ ), respectively [7–10]. If a person is subjected to acoustic noise exceeding these values, it may cause immediate hearing damage and requires actions to make sure that exposure does not happen again. With sound exposure levels exceeding 135 dB(C) (112 Pa) peak SPL and 80 dB (A)  $L_{EX,8h}$ , hearing protection must be available (lower exposure action value), and sound exposures exceeding 137 dB(C) (140 Pa) peak SPL and  $L_{EX,8h}$  of 85 dB(A) make hearing protection mandatory (upper exposure action value). As the TMS coil in a typical experiment is placed near the participant’s ear, the accompanying acoustic noise poses a serious concern on the risk of hearing loss or damage, especially in the case of imperfect hearing protection. Furthermore, acoustic noise causes brain activation through auditory pathways. Therefore, it creates a secondary stimulation mechanism, which can partly mask the effects of the intended neural stimulation caused by the electric field (E-field) induced by the TMS coil [11]. The TMS safety consensus group has suggested

\* Corresponding author. Department of Neuroscience and Biomedical Engineering, Aalto University, Espoo, Finland.

E-mail address: [mikko.nyrhinen@aalto.fi](mailto:mikko.nyrhinen@aalto.fi) (M.J. Nyrhinen).

<https://doi.org/10.1016/j.brs.2024.02.006>

Received 26 April 2023; Received in revised form 10 December 2023; Accepted 8 February 2024

Available online 9 February 2024

1935-861X/© 2024 The Authors. Published by Elsevier Inc. This is an open access article under the CC BY license (<http://creativecommons.org/licenses/by/4.0/>).

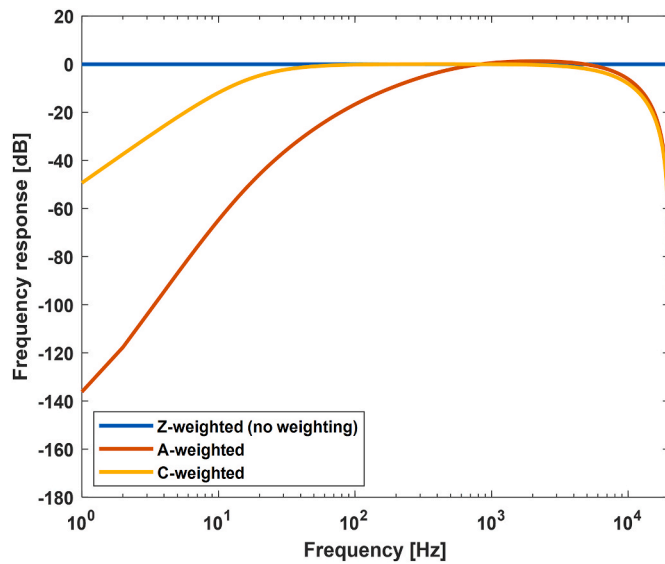


**Fig. 1.** Frequency weightings used in regulations according to standards [9, 10]. A-weighting is usually applied to continuous SPL and C-weighting to impulse SPL measurements to account for the relative loudness perceived by the human ear. The A-weighting is an approximation of the 40-Phon and the C-weighting is an approximation to the 100-Phon equal-loudness contours according to ISO 226:2003 [10].

that measurements of acoustic outputs of new TMS systems are needed and based on the results, safety studies should be conducted [12,13].

Accurately measuring the SPLs of the fast and loud impulse sounds inside an MRI bore is challenging. First, not all decibel meters measure the transient peak sounds but a temporal integral of sound intensity over a short period. These periods called time weightings, are denoted by fast, slow and impulse corresponding to periods of 30, 125 and 1000 ms [14, 15]. To overcome this, it is necessary to use a decibel meter that measures the peak SPL without temporal integral or measure the raw sound using a microphone to avoid any audio pre-processing [16]. Second, most decibel meters, microphones and amplifiers are not MRI-compatible because of ferromagnetic components or components sensitive to magnetic fields. One way to overcome these challenges is to measure the TMS click sounds from a distance and then estimate the SPLs at the TMS coil by assuming that the acoustic noise is attenuated by 6 dB when doubling the distance [17,18]. This method, however, may not be accurate because it assumes the measurement in a spherical

free-field from a point-like source. Also, the acoustic behaviour in the near-field of an acoustic resonator is more erratic than in the far-field [5].

Studies on acoustic outputs of TMS systems and coils [2,3,19–23] and hearing safety [5,19–21] have been reported. However, to our knowledge, no one has measured SPLs of TMS coils inside MRI scanners. In this study, we present a method for measuring the TMS impulse SPLs inside an MRI scanner from the acoustic near-field. We report the SPL measurements of two commercial MRI-compatible TMS systems in the 3-T  $B_0$  field of an MRI scanner. Also, we present the SPL measurements of four commercial TMS stimulators and three different TMS coils in a typical operational environment. These measurements were compared with those outside an MRI system. These findings can guide procedures to protect the safety of participants in TMS and TMS-fMRI experiments against potential hazards to hearing and reduce the confounds in the interpretation of fMRI signals caused by TMS.

## 2. Methods

### 2.1. Acoustic measurements

To accurately measure the SPL of the TMS coil click inside the MRI scanner, we built a system that transmits the sounds generated inside the MRI bore to the outside of the shielding room via a non-elastic tube (Stress Nobel 40 bar, length 6.46 m, diameter 6 mm). The non-elastic tube acts as an acoustic transmission line similar to the human ear canal [24,25]. The sounds were measured with a microphone (MKE-PC2, Sennheiser electronic GmbH & Co. KG, Germany) firmly attached to the end of the tube outside the MRI shielding room. The sounds were recorded using a high-quality audio interface (RME Babyface Pro, Audio AG, Germany) and analysed with a custom MATLAB (Mathworks, Natick, MA, USA) program. The acoustic noise is attenuated, and its spectrum changes when passing through the tube. To characterize this change, a filter was created. A 94-dB SPL/1 kHz calibrator sound (4231 Calibrator, Brüel & Kjær, Denmark) was recorded with a reference microphone (G.R.A.S. 46 A F ½'' Free-field Standard microphone set, capsule) connected to an audio interface (RME fireface 400, Audio AG, Germany). The RMS of this signal was used to estimate a correction coefficient ( $c = 1/\text{RMS}$ ) that ensures a sensitivity of 1 V/Pa for the reference microphone. A sweep sound, ranging from 20 Hz to 20 kHz, was played inside an echoless chamber and the mouth of the tube was installed beside the reference microphone facing a loudspeaker and both microphones were measured (Fig. 2 A). By using a 10-dB gain, we obtained that both microphones have similar levels at frequencies below 200 Hz so the tube and microphone system was normalized so that

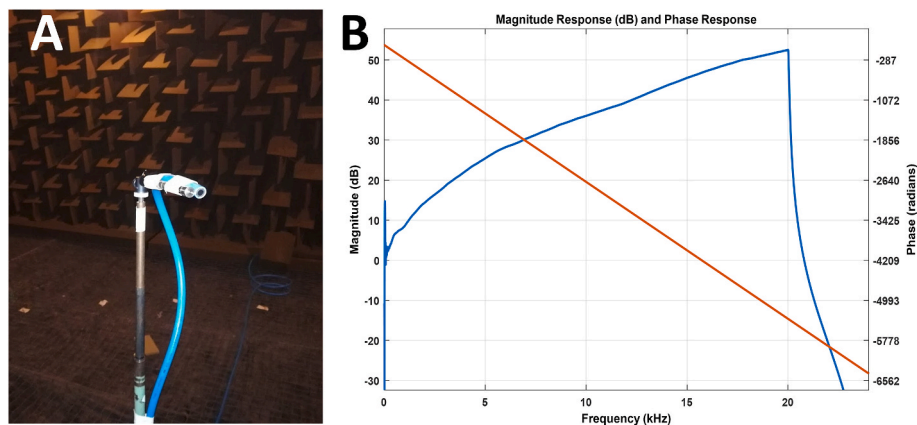


**Fig. 2.** A: Picture of the calibration setup. The calibration measurements of the tube and microphone system were performed in the echoless chambers of Aalto University Department of Signal Processing and Acoustics. The reference microphone is taped next to the open end of the blue tube. B: The magnitude (blue line) and the phase response (red line) of the inverse filter created to account for the effects of the tube. (For interpretation of the references to colour in this figure legend, the reader is referred to the Web version of this article.)

**Table 1**

TMS coils and stimulators, electric fields (E-fields) and corresponding stimulator output (SO). ID is the short identification used in figures and tables. The stimulators and coils are manufactured by Magstim Co. Ltd. (Whitland, UK), Nexstim Plc (Helsinki, Finland) and MagVenture (Farum, Denmark). The MRI scanner was a Siemens Magnetom Skyra 3 T (Germany). The discrepancies between the ratios of numbers in the E-fields and SOs are due to rounding of the numbers.

ID	Stimulator	Coil	E-field [V/m]	SO [%MSO]
R30_MRI	Magventure MagPro R30	MRI-B91	20, 40, 60, 80, 100, 108	19, 37, 56, 74, 93, 100
SPR_MRI	Magstim Super Rapid <sup>2</sup> Plus <sup>1</sup>	MRI D70mm (P/ N: 3310)	20, 40, 60, 80, 100, 120, 128	16, 31, 47, 63, 78, 94, 100
SPR_D70	Magstim Super Rapid <sup>2</sup> Plus <sup>1</sup>	D70mm (P/N: 9925)	60, 100, 140, 151	39, 66, 92, 100
SPR_AIR	Magstim Super Rapid <sup>2</sup> Plus <sup>1</sup>	Air-Cooled D70mm Coil (P/ N3530-00)	20, 60, 100, 125	16, 48, 80, 100
200_D70	Magstim 200 <sup>2</sup>	D70mm (P/N: 9925)	60, 100, 140, 250	24, 40, 56, 100
NBS4	Nexstim NBS 4 System	Nexstim Cooled Coil	60, 100, 140, 230	26, 43, 60, 100
NBS5	Nexstim NBS 5 System	Nexstim Cooled Coil	60, 100, 140, 230	26, 43, 60, 100

frequencies below 200 Hz correspond to 0 dB. Then, the response of the tube and microphone system was flattened by inverting the magnitude response to create the inverse filter, which was then minimum-phase reconstructed. This filter was applied to the acoustic noise measurements of all TMS systems (Table 1). The TMS coil can be oriented arbitrarily inside the MRI relative to the  $B_0$  field but there are three main orientations with distinctively separate force patterns affecting the TMS coil; all the other forces can be derived from these forces [4]. When measuring the sound inside the MRI scanner, the TMS coil was oriented in three ways with respect to the  $B_0$  field, as illustrated in Fig. 3. The TMS click sound was also measured in the absence of the  $B_0$  field outside the scanner. These different setups are referred to as stimulation conditions (Fig. 3).

The SPL behaviour in the near field, where the distance between the sound emitting and receiving device is smaller than twice the largest dimension of the sound emitting device, does not follow the  $1/r$  attenuation rule and there is a chance of underestimating the SPLs [5,22]. On the other hand, measuring from further away does not represent the acoustics near the source. To avoid these complications and to map the SPL spatial distribution, the measurements were taken at different locations and distances from the TMS coil. All measurements were conducted so that the open end of the tube was pointed towards the TMS

coil. The stimulator outputs (SO), induced electric fields, and pulse shapes vary across TMS systems. To compare different combinations of stimulators and coils with a matched stimulation strength, the electric fields induced by TMS systems were measured with a robotic measurement tool [24]. The device enabled automated mapping of the TMS-induced E-field distribution in a spherically symmetric conductor. The maximum stimulator output (MSO) and the corresponding E-field, were derived from an earlier study [24]. If these values were not available, the stimulator output corresponding to 100 V/m E-field was measured using the robotic measurement device [24]. This was the case with MagVenture MagPro R30 (MagVenture, Farum, Denmark) and Nexstim NBS 4 (Nexstim Plc, Helsinki, Finland) systems (Table 1). The other SOs and corresponding E-fields used in this study were calculated by linear interpolation using equation  $E = E_0 \cdot SO/SO_0$ , where the  $SO_0$  is the stimulator output corresponding to  $E_0 = 100$  V/m. At most measurement locations, the stimulation intensity was 100 V/m. At locations  $z = 5$  cm and  $x = 5$  cm, a wider range of stimulation intensities were used (Fig. 3). Combinations of stimulators and TMS coils and SIs used in the measurements are summarized in Table 1. The TMS pulses were delivered with 1–4-s interstimulus intervals. In order to estimate the operator exposure, measurements were conducted using two stimulators Nexstim NBS 5 (Nexstim Plc, Helsinki, Finland) and Magstim Super Rapid<sup>2</sup> Plus<sup>1</sup> (Magstim Co. Ltd., Whitland, UK) (Table 1) with the maximum stimulation output (MSO) using a 40-cm measurement distance from the bottom center of the coil.

2.2. Data analysis

All SPL and equivalent continuous sound level ( $L_{Aeq}$ ) data are expressed as decibels in relation to 20  $\mu$ Pa. All peak SPLs were filtered using C-weighting [9] (Fig. 1), which is used in EU directives [8] and Finnish legislation [7] for assessing the safety of impulse sounds. In TMS pulses, most of the acoustic energy is between 1 and 10 kHz frequency, and, at this range, the C-weighting curve is flat, resulting in SPLs approximately the same as with Z-weightings. The maximum SPLs were calculated as the average across 3–5 impulses. No weighting (Z-weighting) was applied when plotting frequency responses and the TMS click with the median SPL was selected for the analysis. A-weighting [9] was used for the calculation of  $L_{Aeq}$  values. Different  $L_{Aeq}$  values were calculated for commonly used repetitive TMS frequencies (1, 5, 10, 15, and 20 Hz).  $L_{Aeq}$  is a steady sound pressure level over a time window with the same energy as the fluctuating sound, in this case, the measured impulse sound. The  $L_{Aeq}$  was calculated from single-pulse data by selecting a time window of 1/frequency around the TMS impulse and calculating the RMS of the sound pressure. To ensure validity of  $L_{Aeq}$  calculated from single pulse data, TMS stimulation at 10

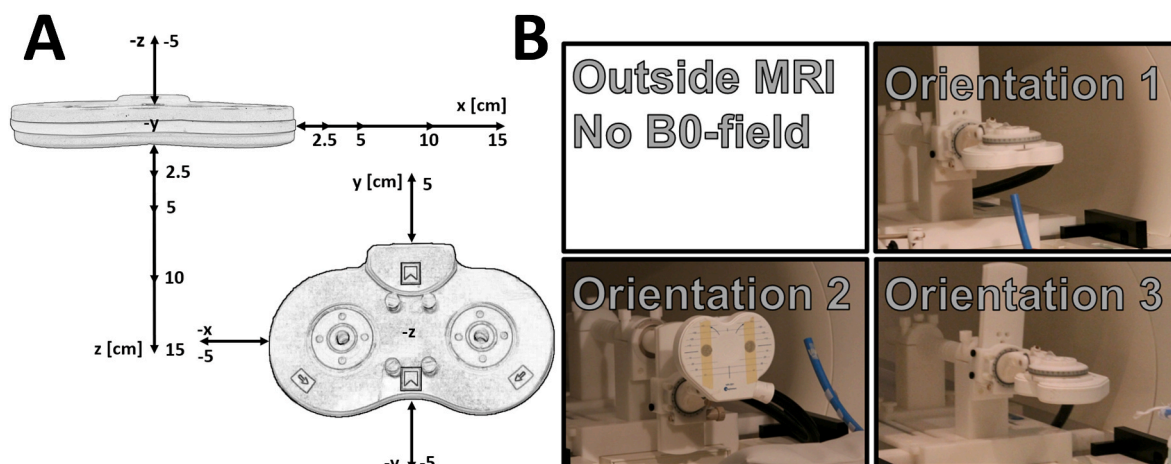


**Fig. 3.** A: Measurement locations of the SPL and the coordinate system. B stimulation conditions, i.e., TMS coil orientations relative to the  $B_0$  field.

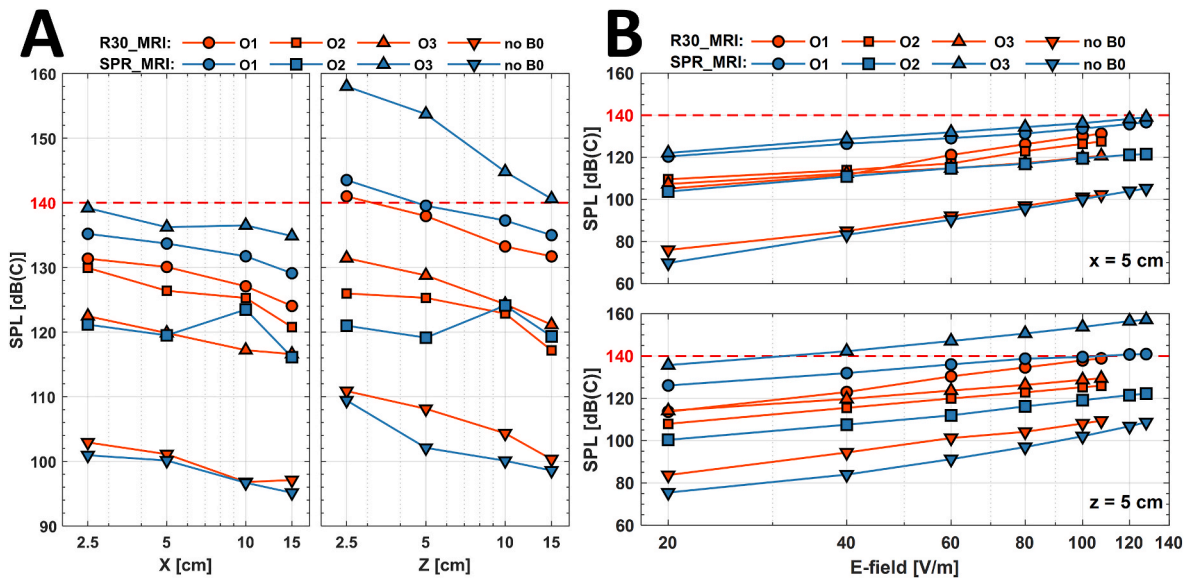


Fig. 4. A: the effect of distance on SPLs of MRI-compatible TMS systems (E-field = 100 V/m). B: the effect of power on SPLs. The dashed redline at 140 dB(C) is the hard exposure limit value for work places. O1, O2 and O3 are orientations 1, 2 and 3.

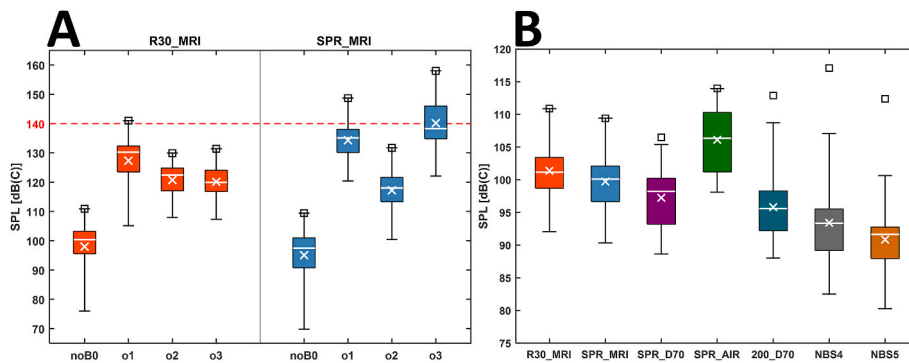


Fig. 5. A: Boxplot of MRI-compatible TMS stimulators for all measurement locations and conditions and matching stimulation intensities (20–100 V/m, degrees of freedom (df) = 159). B: Boxplot of all TMS stimulators outside the B<sub>0</sub> field using all measurement locations and matching (60 and 100 V/m) stimulator intensities (df = 97). Horizontal lines show the median values and crosses show the mean values of the matching stimulation intensities. Maximum SPLs out of all the measurements are marked with squares. The dashed redline at 140 dB(C) is the hard exposure limit value for work places.

Table 2

Maximum SPLs, the coordinate, E-field, and LAeq values of different stimulation frequencies and maximum safe exposure time calculated using the data from the single pulse TMS measurements with the maximum SPL(C). O1-o3 refer to the TMS coil orientations relative to the B<sub>0</sub> field inside the MRI scanner and depicted in Fig. 3. In o1 and o3, the B<sub>0</sub> field is parallel to coil windings and in o2, the B<sub>0</sub> field is perpendicular to the coil windings. Stimulators are not necessarily capable of producing these stimulation frequencies.

Stimulator	Max		Max		1 Hz		5 Hz		10 Hz		15 Hz		20 Hz	
	Coord	E-field	SPL(C)	SPL(Z)	L <sub>Aeq</sub>	t	L <sub>Aeq</sub>	t	L <sub>Aeq</sub>	t	L <sub>Aeq</sub>	t	L <sub>Aeq</sub>	t
	[cm]	[V/m]	[dB]	[dB]	[dB]	[min]	[dB]	[min]	[dB]	[min]	[dB]	[min]	[dB]	[min]
R30_MRI: no B0	z = 2.5	100	111	111	78	3488	85	700	88	350	90	234	91	175
R30_MRI: o1	z = 2.5	100	141	142	107	5	114	1	117	1	118	0	120	0
R30_MRI: o2	x = 2.5	100	130	131	97	52	104	10	107	5	108	3	110	3
R30_MRI: o3	z = 2.5	100	131	132	99	33	106	7	109	3	110	2	112	2
SPR_MRI: noB0	z = 2.5	100	109	111	75	7955	82	1602	85	802	87	535	88	401
SPR_MRI: o1	z = -5.0	100	149	152	112	1	119	0	122	0	124	0	125	0
SPR_MRI: o2	y = 5.0	100	132	133	96	57	103	11	106	6	108	4	109	3
SPR_MRI: o3	z = 2.5	100	158	161	118	0	125	0	128	0	129	0	131	0
SPR_D70	z = 5.0	151	106	110	74	10,131	81	2039	84	1021	85	682	87	513
SPR_AIR	z = 2.5	100	114	115	81	1833	88	367	91	184	93	122	94	92
200_D70	z = 5.0	250	113	115	79	2707	86	557	89	279	91	187	92	141
NBS4	z = 5.0	230	117	119	83	1336	89	275	92	138	94	92	95	69
NBS5	z = 5.0	230	112	114	81	2134	87	489	90	249	92	167	93	126

**Table 3**  
Statistical comparison of MRI compatible TMS stimulators.

Groups		Low CI	Mean	High CI	p-value	
R30_MRI: noB0	R30_MRI: o1	-36.95	-29.36	-21.76	<0.001	*
R30_MRI: noB0	R30_MRI: o2	-30.36	-22.77	-15.17	<0.001	*
R30_MRI: noB0	R30_MRI: o3	-29.73	-22.13	-14.54	<0.001	*
R30_MRI: noB0	SPR_MRI: noB0	-4.68	2.91	10.51	0.942	
R30_MRI: noB0	SPR_MRI: o1	-43.92	-36.32	-28.73	<0.001	*
R30_MRI: noB0	SPR_MRI: o2	-26.83	-19.24	-11.65	<0.001	*
R30_MRI: noB0	SPR_MRI: o3	-49.79	-42.2	-34.6	<0.001	*
R30_MRI: o1	R30_MRI: o2	-1	6.59	14.18	0.145	
R30_MRI: o1	R30_MRI: o3	-0.37	7.22	14.81	0.076	
R30_MRI: o1	SPR_MRI: noB0	24.68	32.27	39.86	<0.001	*
R30_MRI: o1	SPR_MRI: o1	-14.56	-6.97	0.62	0.099	
R30_MRI: o1	SPR_MRI: o2	2.52	10.11	17.7	0.001	*
R30_MRI: o1	SPR_MRI: o3	-20.43	-12.84	-5.25	<0.001	*
R30_MRI: o2	R30_MRI: o3	-6.96	0.63	8.22	1.000	
R30_MRI: o2	SPR_MRI: noB0	18.09	25.68	33.27	<0.001	*
R30_MRI: o2	SPR_MRI: o1	-21.15	-13.56	-5.97	<0.001	*
R30_MRI: o2	SPR_MRI: o2	-4.07	3.52	11.12	0.855	
R30_MRI: o2	SPR_MRI: o3	-27.02	-19.43	-11.84	<0.001	*
R30_MRI: o3	SPR_MRI: noB0	17.46	25.05	32.64	<0.001	*
R30_MRI: o3	SPR_MRI: o1	-21.78	-14.19	-6.6	<0.001	*
R30_MRI: o3	SPR_MRI: o2	-4.7	2.89	10.48	0.944	
R30_MRI: o3	SPR_MRI: o3	-27.65	-20.06	-12.47	<0.001	*
SPR_MRI: noB0	SPR_MRI: o1	-46.83	-39.24	-31.65	<0.001	*
SPR_MRI: noB0	SPR_MRI: o2	-29.75	-22.16	-14.57	<0.001	*
SPR_MRI: noB0	SPR_MRI: o3	-52.7	-45.11	-37.52	<0.001	*
SPR_MRI: o1	SPR_MRI: o2	9.49	17.08	24.67	<0.001	*
SPR_MRI: o1	SPR_MRI: o3	-13.46	-5.87	1.72	0.269	
SPR_MRI: o2	SPR_MRI: o3	-30.55	-22.95	-15.36	<0.001	*

Hz with 5-s duration was also recorded and  $L_{Aeq}$  was calculated by taking the RMS of the entire recording. The maximum exposure time was calculated as  $T_{max} = 480 \text{ min} \cdot 10^{(87-L_{Aeq,t})/10}$ . For the frequency responses, we used a time window of 3 m before the impulse started and 40 m after. This time window approximated the time that the sound waves take to travel back and forth the acoustic measurement tube. The background noise of the same sample size was used to calculate the frequency responses of the background noise. The data samples were single cosine filtered using MATLAB's *Tukeywin* function (Mathworks, Natick, USA) to reduce artifacts arising from cutting the signal. This was then used to create the 1/3 octave spectra, i.e., frequency spectrum was smoothed out to 1/3 octave bands using MATLAB's *p octave* function. The statistical analysis of MRI-compatible stimulators was done by *n*-way analysis of variance (ANOVA), and for all stimulators by a one-way ANOVA. The normality of the distributions was visually inspected using QQ plots. The level for statistical significance was set at 0.05.

### 3. Results

#### 3.1. MRI compatible TMS stimulators and the effect of MRI

MRI compatible TMS stimulators produced noise clicks with varying SPLs (Figs. 4 and 5). The maximum SPL measured at 3 T was 158 dB(C) for the Magstim super rapid plus and MRI D70 coil using orientation 3, and 141 dB(C) for the MagVenture Magpro R30 system (Table 1) with orientation 1 (Table 2, Figs. 4 and 5). In both cases, SPL was measured in

the immediate vicinity at the bottom of the coil ( $z = 2.5 \text{ cm}$ ) with a stimulation intensity of 100 V/m. Outside the MRI bore, the SPLs of the two stimulators were similar peaking at  $\sim 110 \text{ dB}$  (Table 2, Figs. 4 and 5), but inside the MRI bore (with 3 T  $B_0$  field), the Magstim system's maximum SPLs were about 12 dB(C) louder than the Magventure. Across all matching stimulator intensities with the presence of the  $B_0$  field, the Magstim system was about 8 dB(C) louder. The measured SPLs were significantly higher inside the MRI bore compared to outside for MRI-compatible stimulators ( $p < 0.001$ ) (Fig. 5, Table 3). Inside the MRI bore, the MagVenture system had similar SPLs for all TMS coil orientations. In turn, with the Magstim system the TMS coil at orientation 2 had significantly smaller SPLs than at orientations 1 and 3 ( $p < 0.001$ ) (Table 3, Fig. 5). With the TMS coils at orientation 3, the Magstim system produced louder noise clicks than the MagVenture system. The presence of a 3-T magnetic field increased the SPLs on average by 22–29 dB on the MagVenture system and 21–45 dB on the Magstim system depending on the orientation relative to the magnetic field. With the MagVenture system the maximum in the spectra was located at 1000 Hz with all stimulation conditions except with orientation 2, where the maximum shifted to approximately 4000 Hz. (Figs. 6 and 7). With the Magstim system, the maximum was located at 4000 Hz with all stimulation conditions except with orientation 1, where the maximum shifted to approximately 2500 Hz. With both systems, the maximums retained their locations with different stimulation intensities with small fluctuations ( $< 1000 \text{ Hz}$ ) in location. On both systems, doubling the E-field increased the SPLs on average by 8 dB(C). With the presence of a static magnetic field, both stimulators exceeded the 87-dB(A)  $L_{Aeq}$  limit with all orientations, and the maximum exposure time ranged from 0 to 52 min.

#### 3.2. All TMS stimulators outside the MRI

Outside the MRI bore, TMS stimulators produced noise clicks with varying SPLs (Figs. 5 and 8). The maximum SPL measured at 100 V/m was 114 dB(C) with Magstim super rapid plus and air-cooled coil at  $z = 2.5 \text{ cm}$ . The loudest SPL was 117 dB(C) by the Nexstim NBS4 system at the maximum stimulator output (230 V/m) at  $z = 5 \text{ cm}$  (Table 2, Figs. 5 and 8). Outside the MRI bore at 100 V/m, there were statistical differences ( $p < 0.05$ ) in SPLs between systems (Fig. 5, Table 4). In general, the acoustic noise of super rapid plus and the air-cooled coil was statistically different from other system, except with the Magpro R30 system and had the highest SPLs. Also, Nexstim NBS 5 was statistically different from all other systems, except for NBS 4 and Magstim 200 systems, and had the lowest SPLs. The maximum in the spectra was with Magstim super rapid plus and D70 coils, Magstim super rapid plus and air-cooled coil, Magstim 200 and D70 coil, and Nexstim NBS 4 and Nexstim NBS 5, at approximately 6300, 1300, 2000, 7900 and 2500 Hz, respectively (Fig. 9). During the measurements with Nexstim NBS 4 and NBS 5 stimulators, the air cooling had a small effect of the spectra, since the sound level of the cooling is considerably smaller than the acoustic click.

For all systems, the SPLs were, on average, attenuated at longer measurement distances. Across all systems, measurement locations and conditions, the SPLs attenuated 3 dB on average by doubling the distance (Figs. 4 and 8). The measured SPL with Nexstim NBS 5 and Magstim super rapid plus and D70 coil at a 40-cm distance using MSO was both 100 dB(C). The attenuation at a 40-cm compared to a 5-cm distance was 7 dB(C) with Magstim super rapid plus and D70 coils and 12 dB(C) with Nexstim NBS 5 coil. The  $L_{Aeq}$  values ranged from 74 dB(A) to 95 dB(A), and the maximum allowed exposure times ranged from 10,131 min ( $\sim 168 \text{ h}$ ) to 69 min (Table 2). The  $L_{Aeq}$  of 87-dB(A) was exceeded at frequencies of higher than 1 Hz, depending on the stimulator, and the maximum allowed exposure times ranged from 69 to 2039 min ( $\sim 33 \text{ h}$ ).

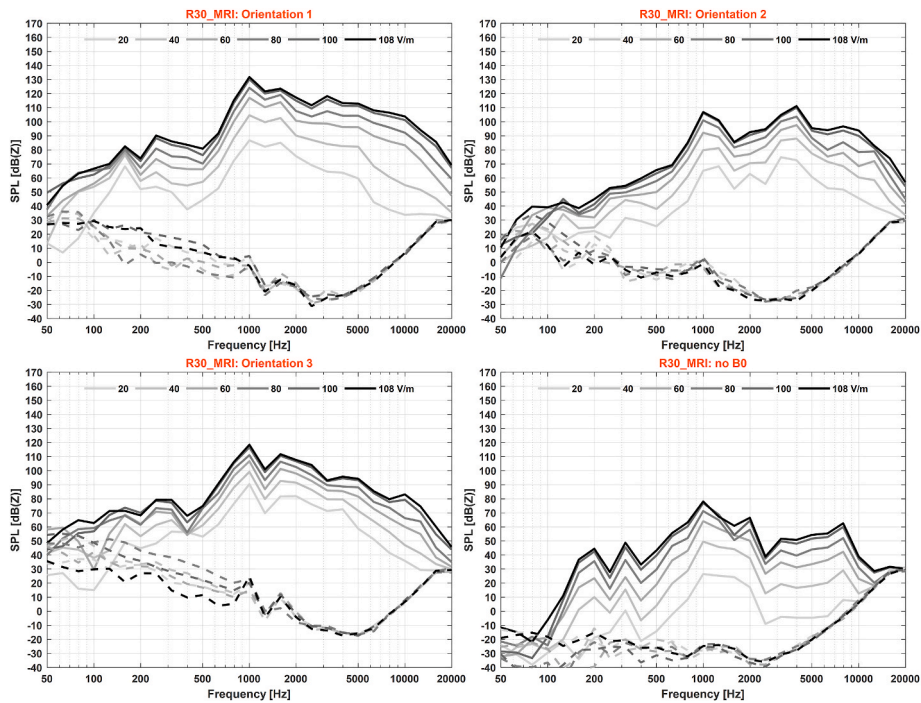


Fig. 6. The 1/3 Octave spectra of MagVenture MagPro R30 stimulator and MRI-B91 coil with different stimulator intensities and orientations. The dashed lines are the ambient noises.

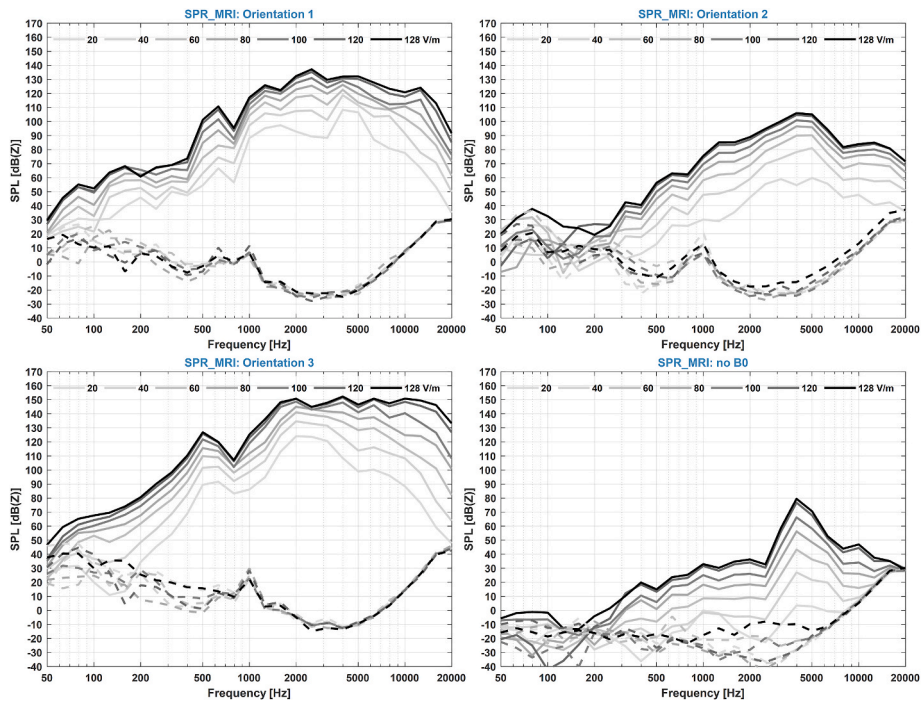


Fig. 7. The 1/3-octave spectra of Magstim super rapid plus stimulator and MRI D70 coil with different stimulator intensities and orientations. The dashed lines are the ambient noises.

#### 4. Discussion

We found that the maximum SPLs increased when the TMS coil was placed inside the MRI and both stimulators exceeded the upper exposure limit (137 dB(C)) and the hard exposure limit (140 dB(C)) for peak SPLs, making the use of hearing protection mandatory. The increase in SPLs was because the current in the coil was subjected to a strong  $B_0$ , which

caused additional Lorentz force over the coil wires. Also, these forces depend on the orientation of the coil windings relative to the  $B_0$  field, as the SPLs changed with different orientations. Interestingly, the two MRI-compatible systems behaved slightly differently under the influence of  $B_0$ . The loudest orientation for the MagVenture system was orientation 1 (141 dB(C)); for the Magstim system, it was orientation 3 (158 dB(C)) (Fig. 5, Table 2). Even though the SPLs outside the MRI bore were very

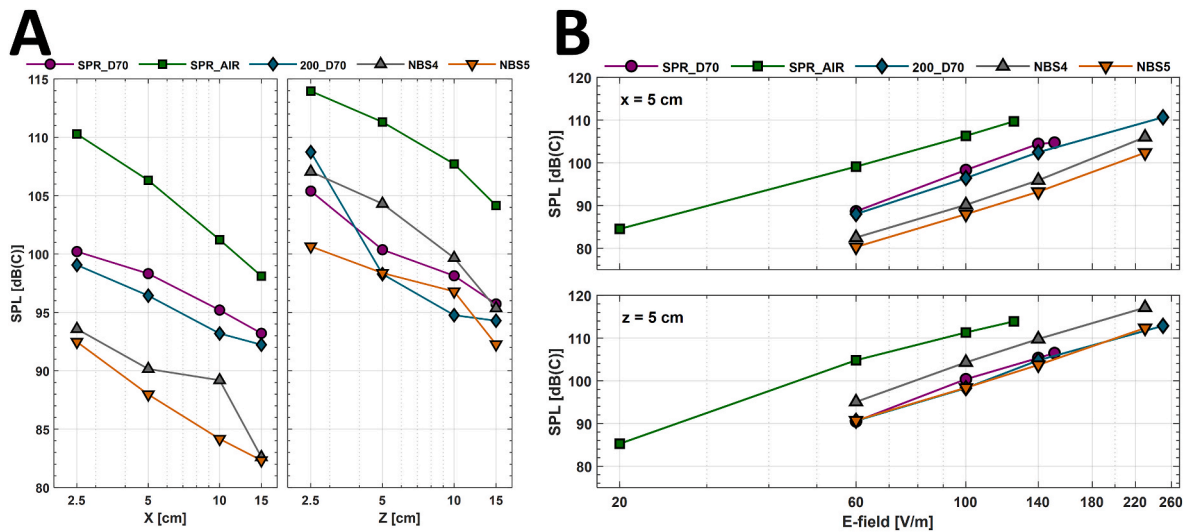


Fig. 8. A: the effect of distance to SPLs of non-MRI compatible TMS-systems (E-field = 100 V/m). B: the effect of stimulus intensity to SPLs with non-MRI-compatible TMS systems.

Table 4

Multiple comparison of the SPLs for all TMS stimulators measured outside the MRI.

Groups	Low CI	Mean	High CI	p-value
R30_MRI SPR_MRI	-4.56	1.66	7.87	0.984
R30_MRI SPR_D70	-2.09	4.13	10.34	0.42
R30_MRI SPR_AIR	-10.95	-4.74	1.48	0.256
R30_MRI 200_D70	-0.65	5.56	11.78	0.11
R30_MRI NBS4	1.74	7.96	14.17	0.004
R30_MRI NBS5	4.32	10.54	16.75	<0.001
SPR_MRI SPR_D70	-3.74	2.47	8.69	0.893
SPR_MRI SPR_AIR	-12.61	-6.39	-0.18	0.04
SPR_MRI 200_D70	-2.31	3.91	10.13	0.488
SPR_MRI NBS4	0.09	6.3	12.52	0.045
SPR_MRI NBS5	2.67	8.88	15.1	<0.001
SPR_D70 SPR_AIR	-15.08	-8.87	-2.65	<0.001
SPR_D70 200_D70	-4.78	1.44	7.65	0.992
SPR_D70 NBS4	-2.39	3.83	10.05	0.513
SPR_D70 NBS5	0.19	6.41	12.63	0.039
SPR_AIR 200_D70	4.08	10.3	16.52	<0.001
SPR_AIR NBS4	6.48	12.7	18.91	<0.001
SPR_AIR NBS5	9.06	15.28	21.49	<0.001
200_D70 NBS4	-3.82	2.39	8.61	0.907
200_D70 NBS5	-1.24	4.97	11.19	0.205
NBS4 NBS5	-3.64	2.58	8.8	0.872

similar to inside the bore, the increased SPLs were higher with Magstim system. Note that the Magstim’s TMS coil in this study was repaired twice during this study, while the MagVenture’s TMS coil remained intact (see Supplementary information). In both repair cases, the top and bottom halves of the Magstim coil housing started to come apart during experiments. Safety limits stated in the user manuals by both manufacturers for operating the TMS coils inside the bore were not exceeded. However, it is important to note that the Magstim stimulator generated ~20 % higher maximum E-field. This may have played a role in the coil durability. Without the  $B_0$ , the SPLs of the two MRI-compatible stimulator had similar SPLs at the matched stimulation intensity of 100 V/m using the non-MRI compatible stimulators (Fig. 5, Table 2). In the near field, the SPLs did not attenuate 6 dB by doubling the distance as typically assumed with point sources (Figs. 4 and 8). In both cases, it the attenuation was 3 dB. We did not notice any clear patterns related to stimulation conditions and axis. This was expected as the dimensions of the coil are larger than the measurement distance to the coil, and therefore, the source was not perceived as a point-like. The attenuation of SPLs from 40 cm to 5 cm distance was 7–12 dB(C), which is less than

the 18 dB(C) (6 dB by doubling the distance) [3] that might be expected if both measurement locations were in spherical free-field. This demonstrates that measurements conducted in far-field might underestimate the SPLs in the acoustic near-field.

In this study, Nexstim NBS 4 and 5 stimulators had the air cooling on during measurements. This has little effect on the maximum SPL. However, cooling affects the spectra (Fig. 9). Interestingly, there are two peaks in the NBS 4 and 5 spectra located at roughly 1000 and 2600 Hz with both the click sound and air cooling. But in the case of the coil click, the SPLs were 20 dB louder, and the peaks remained clearly visible in the spectrum. This cannot be explained by the resonance frequency of the tube, because the calculated resonance frequencies [25] for an open cylindrical tube were below 300 Hz even with the 10th octave harmonics. Thus, peaks were likely originating from the TMS coil click. It makes sense that the vibration of the cooling and vibration caused by the TMS impulse had the same frequencies, since acoustic properties of vibrating objects are partly defined by their shape and size [26]. The Magstim super rapid plus and D70 coils and the Magstim 200 and D70 coils were the same coil but with different stimulators and pulse shapes; Super rapid plus coil used biphasic stimulator and 200 coil used a monophasic stimulator. There were some similarities between the two stimulators, such as the peaks at around 800 and 2000 Hz. However, noticeable differences in the setup highlighted the fact that acoustic spectrum of a TMS system emerges from both the TMS coil properties and TMS current strength. As expected,  $L_{Aeq}$  values increased with the stimulation frequency. Inside the MRI bore, the exposure limit value of 87-dB(A) is exceeded with all stimulators and orientations within 57 min even with the lowest stimulation frequency of 1-Hz (Table 2). Outside the MRI bore, the 87-dBA(A) value was exceeded eventually when stimulation frequency was increased with all the stimulators, showing that hearing protection becomes more important as stimulation frequencies increase.

Previous studies [2,3,19–21] on the acoustic noise of commercial TMS systems utilized different measurement setups (TMS stimulators, measuring distance, frequency weighting, and range), making it challenging to directly compare to our results. Koponen et al. [3] utilized a relatively comparable system with their Magstim rapid<sup>2</sup> and D70 (P/N 9925–00) coil and our Magstim super<sup>2</sup> rapid<sup>1</sup> plus stimulator and D70 coil (Table 2). They observed peak SPLs of about 14–16 dB higher than our measurement at the 5-cm distance [3] and within 2 dB, at 40-cm distance. These differences can be explained by the acoustic behaviour of the near-field measurements. Also, the Magstim D70 (P/N 9925) coils are among the first commercially available figure-of-eight coils

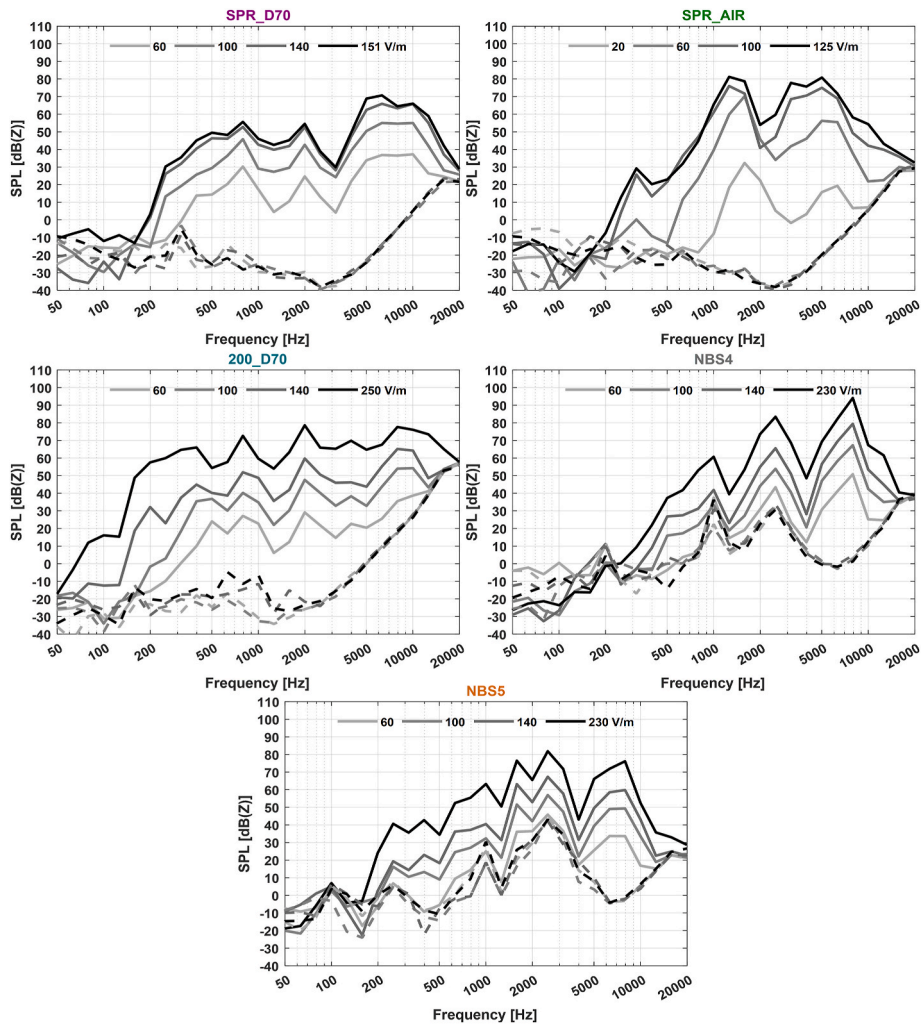


**Fig. 9.** The 1/3-octave spectra of non-MRI compatible TMS systems with different stimulator intensities. The dashed lines are the ambient noises. Note that for NBS 4 and 5 systems the air cooling was on.

produced until the last decade. So, there is a chance that we are compared coils with different wearing due to mechanical stresses. The spectra of the two systems were visually similar. Also, Koponen et al. used the MRI-B91 coil with different stimulator (Magpro X100, MagVenture). If we compared the 100 V/m values, results were within 1 dB difference at the 5-cm distance [3]. Also, both spectra look visually similar (Fig. 6).

We showed the feasibility of our SPL measurement system to measure loud impulse sounds at 3 T. To our knowledge, this is the first study where TMS impulse sounds were measured inside the MRI bore. It is important to point out that in TMS-fMRI, the MRI system also produces continuous acoustic noises generated by gradient coil switching. Previous studies about the acoustic noises of MRI sequences suggest that the LAeq values of echo planar imaging (EPI) sequences used in fMRI are about  $108 \pm 10$  dB (A) in a 3-T magnetic field [27–29]. The total SPL of two sources can be added up together assuming they are not phase locked with an equation  $L_{tot} = 10\log(10^{(L1/10)} + 10^{(L2/10)})$  [30]. In practice, this means that two sources with similar SPLs increase the decibels by 1–3 dB relative to the bigger source, and if the difference between the two sources is greater than 10 dB, the total SPL is approximately the bigger value. As shown in Table 2, the SPL of TMS-fMRI is, in most cases, that of TMS coil clicks. It is also important to notice that imaging sequences and stimulation pulses are usually interleaved and not delivered simultaneously. Therefore, their SPLs can be considered separately. Noise exposures separated by time can be

added together by  $L_{AeqNew} = 10\log(1/(t_1+t_2)(t_1 10^{L_{Aeq1}/10} + t_2 10^{L_{Aeq2}/10}))$ , where  $t_1$  and  $t_2$  are the durations of  $L_{Aeq}$  exposures [31].

The single number ratings (SNR) of hearing protection devices (HPD) and noise reduction ratings (NRR) goes typically up to ~37 dB and ~33 dB respectively [32,33]. These attenuation values given by manufacturers are based on laboratory measurements and do not represent the real attenuation to the user. For example, the U.S. Department of Occupational Safety and Health Administration instructs to calculate the attenuation of HPDs by reducing -7dB from NRR data for A-weighted measurements [34]. The use of double hearing protection adds 5 dB to the larger protection value. Thus, the maximum attenuation is for HPD with NRR of 33 dB is 31 dB. Improper usage of hearing protection can result in significantly smaller SNR/NRR, so it is of utmost importance to ensure that the subjects are instructed about the proper usage of hearing protection. Additionally, researchers should refer to applicable local regulations on how to adjust attenuation label values. But if we assume that the attenuation is 31 dB so, for example, for 10 Hz stimulation frequency, the MagVenture systems  $L_{Aeq} = 117 - 31$  dB = 86 dB, which is more than 9 h of maximum exposure time and for the Magstim MRI-compatible system  $L_{Aeq} = 128 - 31$  dB = 97 dB which is about 50 min of exposure time. The operation of TMS coils in 3-T MRI scanners poses serious risks to hearing safety when using the Magstim TMS device, even if using hearing protection. Also, acoustic noise is not just a hearing safety concern; exposure to noise can cause many non-auditory

effects on humans, for example, annoyance, ischemic heart disease, hypertension, sleep disturbance, changes in the immune system, and birth defects [35]. Furthermore, the acoustic noise of the TMS click leads to confounding neural effects by activating the auditory cortex [5], which can be hard to distinguish from the evoked activity, for instance, in concurrent TMS and electroencephalography (TMS–EEG). Furthermore, the forces on the TMS coil depend on coil orientation with respect to the static magnetic field of the MRI and therefore causes orientation-dependent auditory stimulation. In TMS–EEG the auditory evoked potential (AEP) is removed by masking the click sound with noise [11]. Unfortunately, in many cases it is not possible to remove the auditory component during TMS–fMRI by using the combination of noise masking and hearing protection. It is possible to use active noise cancellation (ANC) to reduce the MRI acoustic noise levels [36] but it works only on continuous low-frequency sounds and therefore does not work on TMS impulse sounds. Using a multi-channel TMS [37,38] with electronic control of stimulus orientation might allow positioning of the TMS coil such that the SPLs are minimized while still enabling changing the stimulus orientation induced in the cortical surface.

Because of the limited number of measurement locations in the near-field, we cannot confidently state that the measured SPLs are the maximum possible SPL created by the stimulators. In the near-field, the acoustic behaviour may be erratic, and we may have measured the SPL from a spatial valley point and not the peak locations. Thus, we can only state that the SPLs are at least what we measured in this article and might be higher in neighboring locations. In the future, more measurement locations should be explored for a comprehensive mapping of the SPL spatial distribution in the near-field. Also, we only measured airborne sound and not the transfer of acoustic energy through the skull [5]. Also, the TMS coils were measured in normal operation environment including the ambient noise and the sound due to the TMS electronics. Finally, the TMS coil orientations compared to the  $B_0$ -field used in this study may be unsuitable for a human TMS–fMRI experiments, however, they were selected to obtain the full range of SPLs resulting from the strongest and weakest Lorentzian forces between the coil current and the static magnetic field. Knowing this range is necessary for a more comprehensive evaluation of the safety risks involved in the technique.

## 5. Conclusion

Hearing protection is obligatory during concurrent TMS–fMRI experiments to ensure safety and it is highly recommended during any TMS experiments. Based on our measurements, we recommend that hearing protection should be available for researchers and subjects, who should be informed about their proper use. More studies about the effects of acoustic noise on hearing is recommended. The manufacturing of quieter TMS systems is encouraged to reduce the risk of hearing damage and other unwanted effects.

## CRedit authorship contribution statement

**Mikko J. Nyrhinen:** Conceptualization, Data curation, Formal analysis, Investigation, Methodology, Software, Visualization, Writing – original draft, Writing – review & editing. **Victor H. Souza:** Conceptualization, Investigation, Methodology, Visualization, Writing – review & editing. **Risto J. Ilmoniemi:** Conceptualization, Funding acquisition, Methodology, Resources, Supervision, Writing – review & editing. **Fa-Hsuan Lin:** Conceptualization, Funding acquisition, Methodology, Resources, Supervision, Writing – review & editing.

## Declaration of competing interest

Risto J. Ilmoniemi is founder, past CEO, advisor, and a minority shareholder of Nexstim Plc. The other authors declare no conflict of interest.

## Acknowledgments

Special thanks to Javier Gómez Bolaños from the Aalto University Department of Signal Processing and Acoustics for helping to set up the measurement system. This work was supported by the Academy of Finland (Nos. 298131 and 349985), Jane and Aatos Erkkö Foundation (A new era in brain stimulation: development of next-generation EEG/fMRI compatible multi-channel brain stimulation technology), Instrumentarium Science Foundation (Aivojen kuvantamisen ja stimulaation yhdistäminen), Natural Sciences and Engineering Research Council of Canada (NSERC; RGPIN-2020-05927), Canada Foundation for Innovation (38913 and 41351), Canadian Institutes of Health Research (PJT 178345), and MITACS (IT25405). This project has received funding from the European Research Council (ERC) under the European Union's Horizon 2020 research and innovation programme (grant agreement No 810377).

## Appendix A. Supplementary data

Supplementary data to this article can be found online at <https://doi.org/10.1016/j.brs.2024.02.006>.

## References

- [1] Nikouline V, Ruohonen J, Ilmoniemi RJ. The role of the coil click in TMS assessed with simultaneous EEG. *Clin Neurophysiol* 1999;110:1325–8. [https://doi.org/10.1016/S1388-2457\(99\)00070-X](https://doi.org/10.1016/S1388-2457(99)00070-X).
- [2] Dhamne SC, Kothare RS, Yu C, Hsieh T-H, Anastasio EM, Oberman L, et al. A measure of acoustic noise generated from transcranial magnetic stimulation coils. *Brain Stimul* 2014;7:432–4. <https://doi.org/10.1016/j.brs.2014.01.056>.
- [3] Koponen LM, Goetz SM, Tucci DL, Peterchev AV. Sound comparison of seven TMS coils at matched stimulation strength. *Brain Stimul* 2020;13:873–80. <https://doi.org/10.1016/j.brs.2020.03.004>.
- [4] Bungert A. TMS combined with fMRI. Thesis. University of Nottingham; 2010.
- [5] Goetz SM, Lisanby SH, Murphy DLK, Price RJ, O'Grady G, Peterchev AV. Impulse noise of transcranial magnetic stimulation: measurement, safety, and auditory neuromodulation. *Brain Stimul* 2015;8:161–3. <https://doi.org/10.1016/j.brs.2014.10.010>.
- [6] Mizutani-Tiebel Y, Tik M, Chang K-Y, Padberg F, Soldini A, Wilkinson Z, et al. Concurrent TMS–fMRI: technical challenges, developments, and overview of previous studies. *Front Psychiatr* 2022;13:825205. <https://doi.org/10.3389/fpsy.2022.825205>.
- [7] FINLEX® - Säädökset alkuperäisinä. Valtioneuvoston asetus työnteekijöiden suojelemisesta melusta aiheutuvilta vaaroilta 85/2006. Oikeusministeriö; 2006.
- [8] Directive 2003/10/EC of the European Parliament and of the Council of 6 February 2003 on the minimum health and safety requirements regarding the exposure of workers to the risks arising from physical agents (noise) (Seventeenth individual Directive within the meaning of Article 16(1) of Directive 89/391/EEC). OJ L; 2003.
- [9] ANSI/ASA S1.4-2014/Part 1/IEC 61672-1:2013. American national standard. Electroacoustics – sound level meters – Part 1: specifications (a nationally adopted international standard). 2014.
- [10] ISO 226:2023 Acoustics — Normal equal-loudness-level contours 2023.
- [11] Russo S, Sarasso S, Puglisi GE, Dal Palù D, Pigorini A, Casarotto S, et al. TAAC - TMS Adaptable Auditory Control: A universal tool to mask TMS clicks. *J Neurosci Methods* 2022;370:109491. <https://doi.org/10.1016/j.jneumeth.2022.109491>.
- [12] Rossi S, Hallett M, Rossini PM, Pascual-Leone A. Safety, ethical considerations, and application guidelines for the use of transcranial magnetic stimulation in clinical practice and research. *Clin Neurophysiol* 2009;120. <https://doi.org/10.1016/j.clinph.2009.08.016>. 2008–39.
- [13] Rossi S, Antal A, Bestmann S, Bikson M, Brewer C, Brockmüller J, et al. Safety and recommendations for TMS use in healthy subjects and patient populations, with updates on training, ethical and regulatory issues: Expert Guidelines. *Clin Neurophysiol* 2021;132:269–306. <https://doi.org/10.1016/j.clinph.2020.10.003>.
- [14] Sound Level Meter Time Weightings - Fast, Slow or Impulse? n.d. <https://noisemeters.com/help/faq/time-weighting/> (accessed February 1, 2023).
- [15] Decibel Meter PCE-MSL 1 | PCE Instruments n.d. [https://www.pce-instruments.com/eu/measuring-instruments/test-meters/decibel-meter-pce-instruments-decibel-meter-pce-1-det\\_5971831.htm](https://www.pce-instruments.com/eu/measuring-instruments/test-meters/decibel-meter-pce-instruments-decibel-meter-pce-1-det_5971831.htm) (accessed February 2, 2023).
- [16] Class 2 Data Logging Decibel Meter PCE-428-ICA incl. ISO Calibration Cert. | PCE Instruments n.d. [https://www.pce-instruments.com/eu/measuring-instruments/test-meters/decibel-meter-pce-instruments-class-2-data-logging-decibel-meter-pce-428-ica-incl-iso-calibration-cert-det\\_5975791.htm](https://www.pce-instruments.com/eu/measuring-instruments/test-meters/decibel-meter-pce-instruments-class-2-data-logging-decibel-meter-pce-428-ica-incl-iso-calibration-cert-det_5975791.htm) (accessed February 2, 2023).
- [17] Hongisto V, Oliva D. Tuulivoimaloiden infraäänit ja niiden terveysvaikutukset n.d.
- [18] Sound Propagation - the Inverse Square Law n.d. [https://www.engineeringtoolbox.com/inverse-square-law-d\\_890.html](https://www.engineeringtoolbox.com/inverse-square-law-d_890.html) (accessed September 4, 2023).

- [19] Tringali S, Perrot X, Collet L, Moulin A. Repetitive transcranial magnetic stimulation: hearing safety considerations. *Brain Stimul* 2012;5:354–63. <https://doi.org/10.1016/j.brs.2011.06.005>.
- [20] Kukke SN, Brewer CC, Zalewski C, King KA, Damiano D, Alter KE, et al. Hearing safety from single- and double-pulse transcranial magnetic stimulation in children and young adults. *J Clin Neurophysiol Off Publ Am Electroencephalogr Soc* 2017;34:340–7. <https://doi.org/10.1097/WNP.0000000000000372>.
- [21] Schraven SP, Plontke SK, Rahne T, Wasserka B, Plewnia C. Hearing safety of long-term treatment with theta burst stimulation. *Brain Stimul* 2013;6:563–8. <https://doi.org/10.1016/j.brs.2012.10.005>.
- [22] Goetz SM, Murphy DLK, Peterchev AV. Transcranial magnetic stimulation device with reduced acoustic noise. *IEEE Magn Lett* 2014;5:1–4. <https://doi.org/10.1109/LMAG.2014.2351776>.
- [23] Koponen LM, Goetz S, Peterchev AV. Double-containment coil with enhanced winding mounting for transcranial magnetic stimulation with reduced acoustic noise. *IEEE Trans Biomed Eng* 2020. <https://doi.org/10.1109/TBME.2020.3048321>. 1–1.
- [24] Nieminen JO, Koponen LM, Ilmoniemi RJ. Experimental characterization of the electric field distribution induced by TMS devices. *Brain Stimul* 2015;8:582–9. <https://doi.org/10.1016/j.brs.2015.01.004>.
- [25] Hiipakka M. Measurement apparatus and modelling techniques of ear canal acoustics. MSc thesis. Espoo: Helsinki University of Technology; 2008.
- [26] Prezelj J, Lipar P, Belšak A, Čudina M. On acoustic very near field measurements. *Mech Syst Signal Process* 2013;40:194–207. <https://doi.org/10.1016/j.ymssp.2013.05.008>.
- [27] Foster JR, Hall DA, Summerfield AQ, Palmer AR, Bowtell RW. Sound-level measurements and calculations of safe noise dosage during EPI at 3 T. *J Magn Reson Imag* 2000;12:157–63. [https://doi.org/10.1002/1522-2586\(200007\)12:1<157::AID-JMRI17>3.0.CO;2-M](https://doi.org/10.1002/1522-2586(200007)12:1<157::AID-JMRI17>3.0.CO;2-M).
- [28] Ravicz ME, Melcher JR, Kiang NY-S. Acoustic noise during functional magnetic resonance imaging. *J Acoust Soc Am* 2000;108:1683–96.
- [29] AMI centre facilities - miscellaneous. Aalto University, <https://www.aalto.fi/en/aalto-neuroimaging-ani-infrastructure/ami-centre-facilities-miscellaneous>. [Accessed 18 August 2023].
- [30] Adding acoustic levels summing sound levels 10 combining addition summation sum decibel levels or SPL of up to ten incoherent sound sources audio logarithmic decibel scale identical summing 1/3 octave spl full octave sum sound pressure level noise sound pressure acoustic pressure volts - sengpielaudio Sengpiel Berlin n.d. <http://www.sengpielaudio.com/calculator-spl.htm> (accessed August 30, 2023).
- [31] Sound -  $L_{eq}$  - Equivalent Level n.d. [https://www.engineeringtoolbox.com/equivalent-sound-level-d\\_721.html](https://www.engineeringtoolbox.com/equivalent-sound-level-d_721.html) (accessed August 25, 2023).
- [32] 3M™ E-A-Rsoft™ FX Earplugs n.d. [https://www.3m.co.uk/3M/en\\_GB/p/d/b00017634/](https://www.3m.co.uk/3M/en_GB/p/d/b00017634/) (accessed August 17, 2023).
- [33] 3MTM E-A-Rsoft™ Yellow Neons™ Earplugs n.d. [https://www.3m.com/3M/en\\_US/p/d/b00017636/](https://www.3m.com/3M/en_US/p/d/b00017636/) (accessed August 17, 2023).
- [34] Occupational Safety and Health Administration, U.S. Department of Labor. OSHA Technical Manual (OTM) Section III: Chapter 5 n.d. <https://www.osha.gov/otm/section-3-health-hazards/chapter-5>.
- [35] Passchier-Vermeer W, Passchier WF. Noise exposure and public Health n.d.:vol. 9.
- [36] McJury MJ. Acoustic noise and magnetic resonance imaging: a narrative/descriptive review. *J Magn Reson Imag* 2022;55:337–46. n.d./n/a, <https://doi.org/10.1002/jmri.27525>.
- [37] Souza VH, Nieminen JO, Tugin S, Koponen LM, Baffa O, Ilmoniemi RJ. TMS with fast and accurate electronic control: measuring the orientation sensitivity of corticomotor pathways. *Brain Stimul* 2022;15:306–15. <https://doi.org/10.1016/j.brs.2022.01.009>.
- [38] Nieminen JO, Sinisalo H, Souza VH, Malmi M, Yuryev M, Tervo AE, et al. Multi-locus transcranial magnetic stimulation system for electronically targeted brain stimulation. *Brain Stimul* 2022;15:116–24. <https://doi.org/10.1016/j.brs.2021.11.014>.